Vietnam Journal of Catalysis and Adsorption
Tạp chí xúc tác và hấp phụ Việt Nam

http://chemeng.hust.edu.vn/jca/

# Preparation of $MoS_2$ nano-corals by hydrothermal method for adsorption of tartrazine in the aqueous medium

Mac Van Hung and Vu Anh Tuan*

*School of Chemical Engineering, Hanoi University of Science and Technology, Hanoi, Vietnam*
**Email: tuan.vuanh@hust.edu.vn*

ARTICLE INFO

Received: 13/10/2020
Accepted: 30/12/2020

*Keywords:*
$MoS_2$, Hydrothermal, Tartrazine, Adsorption, Water treatment, Tartrazine

ABSTRACT

Corals-like molybdenum disulfide ($MoS_2$) have been successfully synthesized via the hydrothermal method. The as-prepared $MoS_2$ material with a high surface area of 83.9 $m^2.g^{-1}$ was used for the removal of tartrazine from an aqueous solution. The effects of parameters including contact time, $MoS_2$ dosage, and solution pH on adsorption capacity were studied. The optimal dosage of $MoS_2$ for removing tartrazine was 0.08 g and the removal efficiency of tartrazine reached 81.5 % for 100 min of adsorption. The adsorption kinetics studies were carried out using pseudo-first-order, pseudo-second-order, and intra-particle diffusion models. The results showed that the pseudo-second-kinetic model better described the adsorption kinetics of tartrazine on $MoS_2$ and film diffusion was the rate-limiting step. In addition, the adsorption capacity of $MoS_2$ was also performed with various organic dyes such as nile blue, janus green B, and congo red.

## Introduction

Organic synthetic dyes have played a key role in industrial production of fabrics, coatings, and pigments. Today, at least 100,000 different types of dyes have been used in industries [1], a certain amount of these dyes is released into the environment during use. They have great effects on human health and ecosystems. Therefore, the removal of organic dyes in wastewater from factories before being discharged into the environment is necessary. Currently, scientists have found many methods to remove dyes such as precipitation, adsorption, ion exchange, chemical oxidation, biological degradation, and coagulation [2]. In which, adsorption is believed to be a low-cost and rapid method for effective removal of organic dyes and has been widely used in water treatment.

Tartrazine is confirmed to be highly toxic for humans as it causes asthma, eczema, thyroid cancer, and some other behavioral problems [3].

Molybdenum disulfide ($MoS_2$) is a typical layered transition metal dichalcogenide formed by the stacking of weakly interacting 2D S-Mo-S layer like graphite. It shows many potential applications resulting from its excellent electrochemical, mechanical, and optical properties [4]. Recently, $MoS_2$ has been used as solid material lubricants [5], photocatalyst for hydrogen generation, and water treatment [6, 7], boosting lithium storage capability [8].

In this study, $MoS_2$ nano-corals were synthesized by the hydrothermal method. As-synthesized sample was characterized by XRD, BET, FE-SEM, and FT-IR. The adsorption performance of sample was evaluated by removal of dyes. Also, the effects of contact time, the

http://doi.org/10.51316/jca.2020.076

dosage of $MoS_2$, and pH solution on adsorption of dye and adsorption kinetics were studied.

## Experimental

### *Materials*

Thioacetamide ($C_2H_5NS$, 99%) and sodium molybdate dihydrate ($Na_2MoO_4.2H_2O$, 99%) were purchased from China. Tartrazine, methylene blue, congo red, and janus green B were purchased from Sigma-Aldrich. All the chemicals were used without any purification. Distilled water was used throughout the experiments.

### *Synthesis of $MoS_2$*

$MoS_2$ nano-corals were synthesized via a simple hydrothermal method using sodium molybdate dihydrate ($Na_2MoO_4.2H_2O$) and thioacetamide ($C_2H_5NS$) as starting materials. In the first stage, 0.54 g of $Na_2MoO_4.2H_2O$ and 0.36 g of $C_2H_5NS$ were dissolved in 40 mL of distilled water. After stirring for about 60 min, the solution was poured into a 100 mL Teflon-lined stainless steel autoclave and then heated at 200 °C for 48h. Subsequently, the autoclave was cooled to room temperature, the precipitation was detached by vacuum pumping filtration, washed with distilled water and ethanol for 3-4 times, and dried at 70 °C for 12h.

### *Adsorption experiment*

Bath adsorption was carried out at room temperature by adding certain amount of $MoS_2$ to a beaker containing 100 mL dye solution of desired concentration under magnetic stirring. At the various time intervals, aliquot of solution about 2 mL was filtered to analyze the dye concentration by the UV-vis spectrophotometer (Agilent 8453). The equilibrium adsorption capacity ($q_e$) and the removal efficiency (Re) of dyes were determined by equations (1) and (2), respectively.

$$q_e = \frac{(C_o - C_e) \times V}{m} \quad (1)$$

$$Re = \frac{C_o - C_t}{C_o} \times 100\% \quad (2)$$

where $q_e$ (mg/g) is the equilibrium adsorption amount, $C_o$ (mg/L), $C_e$ (mg/L) and $C_t$ is the initial, equilibrium and concentration at t time, respectively; V (L) is the solution volume and m (g) is the mass of adsorbent.

### *Characterization of materials*

The crystalline phase of as-prepared $MoS_2$ was investigated by X-ray power diffraction. XRD patterns were obtained by using Bruker D8 Ax XRD-diffractometer (Germany) with $CuK_\alpha$ irradiation (40kV, 40 mA). The 2θ ranging from 20 to 80° was selected to analyze the crystal structure. Fourier transform infrared (FT-IR) spectra were recorded on JASCO FT/IR-4600 spectrometric analyzer. The sample morphology was observed via scanning electron microscopy (FE-SEM, JEOL-7600F) operated at 15 kV. Textural properties were measured via $N_2$ adsorption/desorption isotherm using a Quantachrome instrument (Autosorb iQ, version 3.0 analyzer). The specific surface area was calculated by using the Brunauer-Emmett-Teller (BET) method and the pore size distribution was obtained by using the Barrett-Joyner-Halenda (BJH) method.

### *Adsorption kinetics*

The study of chemical kinetics can provide important information on adsorption rate and the factors affect the adsorption rate. The adsorption kinetic experiments were carried out in the bath model by taking 0.08 g of $MoS_2$ powder to 100 mL of 20 mg/L tartrazine solution at room temperature.

To assess the dynamic characteristics, pseudo-first-order and pseudo-second-order kinetic equations (equations (3) and (4)) were applied to fit the experimental data linearly.

$$\ln(q_e - q_t) = \ln q_e - k_1.t \quad (3)$$

$$\frac{t}{q_t} = \frac{1}{k_2 q_e^2} + \frac{t}{q_e} \quad (4)$$

where $q_t$ and $q_e$ are the amount of tartrazine adsorbed (mg/g) at time t and equilibrium, respectively. $k_1$ ($min^{-1}$) is the rate constant of the pseudo-first-order kinetic model and $k_2$ ($g.mg^{-1}.min^{-1}$) is the rate constant of the pseudo-second-order kinetic model.

In order to understand the diffusion mechanism, the intra-particle diffusion kinetic model was tested by using Weber-Morri' equation [9] which describes dye uptake and varies almost proportionally with $t^{0.5}$ rather than with the contact time t.

$$q_t = k_i.t^{0.5} + C \quad (5)$$

Where $q_t$ (mg/g) is the quantity of dye ions adsorbed at time t, $k_i$ ($mg.g^{-1}.min^{-0.5}$) is the intraparticle diffusion rate constant, and C is thickness of the boundary layer. The larger C implies the greater effect of the boundary layer. According to the model, the adsorption process is controlled by the intra-particle diffusion model if the plot of qt versus $t^{0.5}$ is a straight line passing through the origin.

## Result and discussion

### *Characterization of materials*

The XRD pattern of $MoS_2$ was recorded and is presented in Figure 1 (a). The diffraction peaks of $MoS_2$ matched the standard peaks of $MoS_2$ hexagonal structure (JCPDS no. 87-2416) and the characteristic diffraction peaks at 2θ = 33.28°, 39.58°, and 58.76° could be assigned to the network planes (100), (103) and (110) [10].

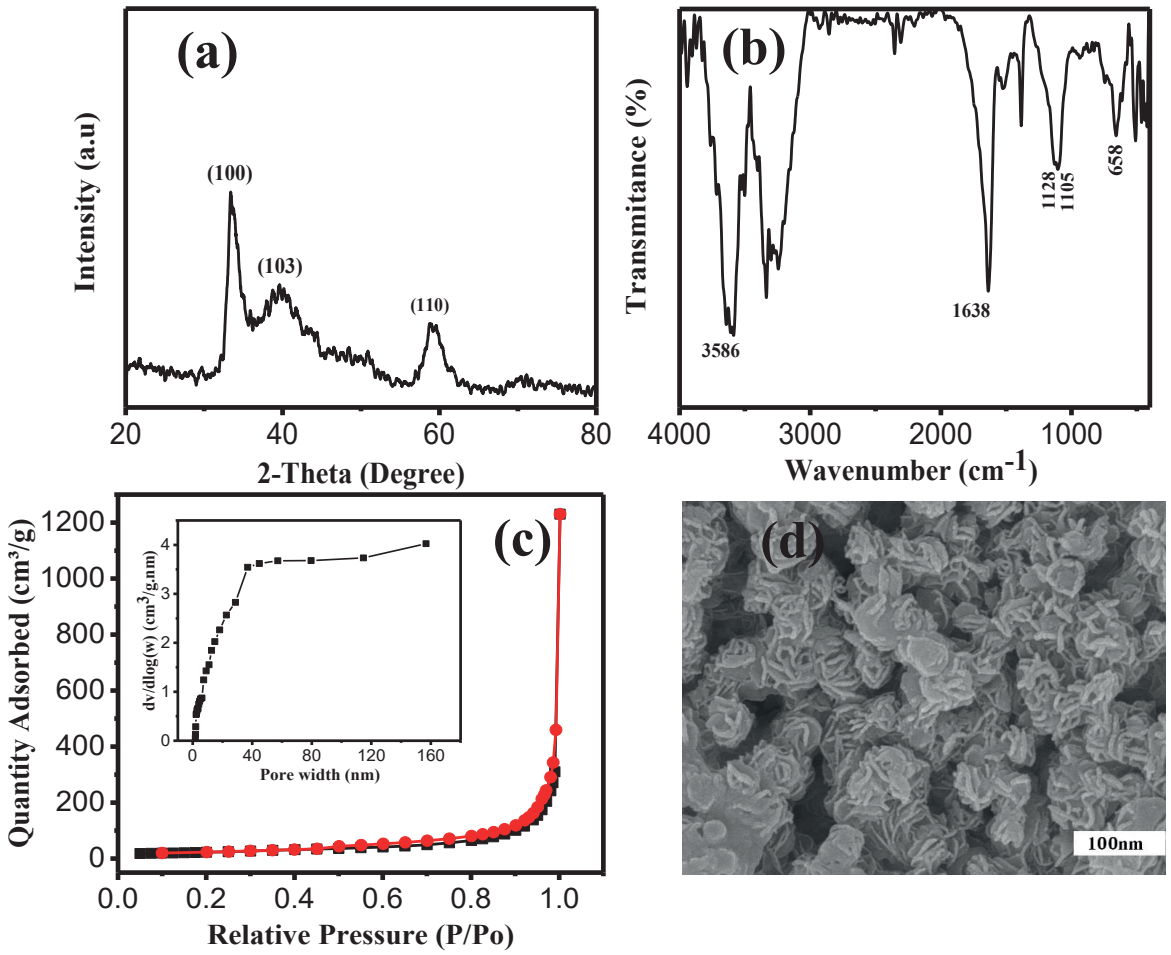


Figure 1: Characterization of as-prepared $MoS_2$, XRD pattern (a), FT-IR spectra (b), $N_2$ adsorption/desorption isotherm and pore size distribution (c) and SEM image (d), respectively

The FT-IR spectrum of as-synthesized $MoS_2$ is shown in Figure 1(b). The strong band at 3586 $cm^{-1}$ corresponded to the vibration of O–H bonding in adsorbed water (H–O–H) on the surface of $MoS_2$. The strong band at 1638 $cm^{-1}$ was assigned to the C=O valence oscillation bond of the carboxyl group (–COOH) [11]. The band at 1128 $cm^{-1}$ was assigned to the oscillation of the S=O bond in $MoS_2$. Finally, the band at 658 $cm^{-1}$ could be assigned to the characteristic of the bending oscillation of $S_xO_y$ [12]. Typical $N_2$ adsorption/desorption isotherm and pore size distribution of $MoS_2$ sample are shown in Figure 1(c). The isotherm was classified as type IV. When the relative pressure ($p/p_o$) increased from 0.91 to 0.98, the hysteresis loop was observed. In addition, when the relative pressure was higher than 0.98 a sudden increase in nitrogen adsorption was observed. These revealed the presence of mesopore. The capillary size distribution of the $MoS_2$ material was relatively broad showing the average pore diameter of 18.9 nm. The pore volume was 0.48 $cm^3/g$ and the BET specific surface area was 83.9 $m^3/g$ as shown in Table 1.

The SEM image of $MoS_2$ is shown in Figure 1(d). The $MoS_2$ was observe as the coral-like shape. It was combined from many nano-sheets at the thickness of about 10 nm. It resulted in the larger pore in the sample and the relatively high surface area (in Table 1). These could be significant factor for accelerating the

adsorption capacity and adsorption rate of dyes on $MoS_2$.

Table 1. Parameters of the BET analysis results of $MoS_2$ material.

| Sample | $S_{BET}$ ($m^2/g$) | $V_{Pore}$ ($cm^3/g$) | $d_{Pore}$ (nm) |
|---|---|---|---|
| $MoS_2$ | 83.9 | 0.48 | 18.9 |

*Adsorption experiment*

*Effect of $MoS_2$ dosage on adsorption of tartrazine*

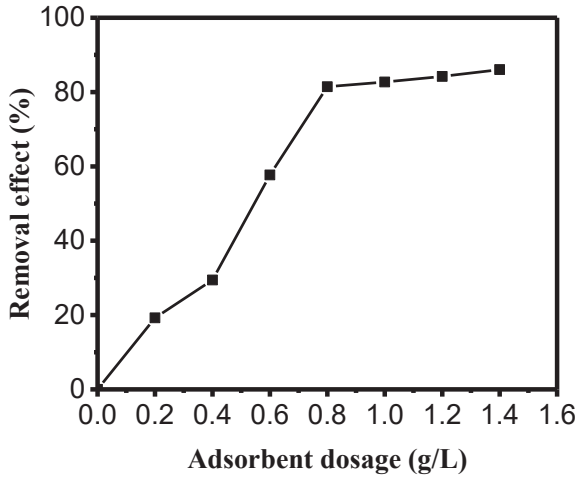


Figure 2: Effect of $MoS_2$ dosage on adsorption of tartrazine

To obtain the optimal adsorbent dosage for the removal of tartrazine, different dosage levels of $MoS_2$ were ranged from 0.2 to 1.4 g/L. The tartrazine concentration was 20 mg/L, the temperature and pH solution were 30 °C and 7.0, respectively, for all the experiments.

The experiment results were shown in Figure 2. As the dosage of $MoS_2$ increased from 0.2 g/L to 0.8 g/L, the adsorption removal ratios significantly increased from 19.3% to 81.5%. However, when the dosage increased from 0.8 g/l to 1.4 g/L, the removal efficiency slightly increased from 81.5% to 86.1%. Since, the adsorption capacity is the crucial factor for an adsorption process, the adsorbent dosage at 0.8 g/L was used for further experiments.

*Effect of contact time on adsorption of tartrazine*

The effect of contact time on adsorption of tartrazine was investigated by adding 0.08 g of $MoS_2$ to 100 mL of 20 mg/L dye solution (pH = 7.0 and 30 °C) and the whole solution was slowly stirred. The tartrazine concentration was detected at different time intervals in the range of 0-120 min and the result is are shown in Figure 3. It can be seen that the tartrazine removal efficiency rapidly increased to 45.0% in the initial 10 min, then slowly increased to 81.5% in 100 min. The adsorption rate did not change and the equilibrium was established at 120 min. It was selected for the subsequent adsorption experiments.

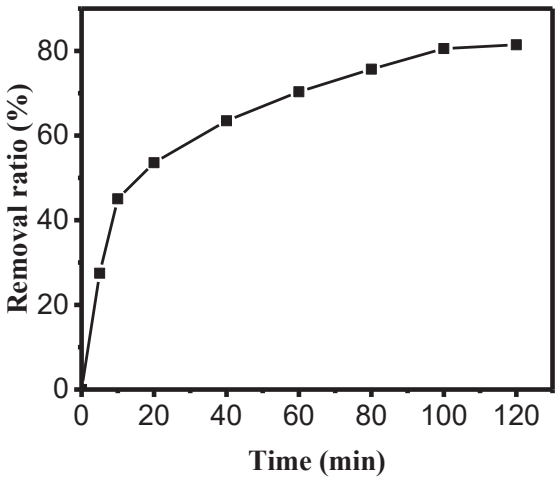


Figure 3: Effect of contact time on dye removal efficiency.

*Effect of solution pH*

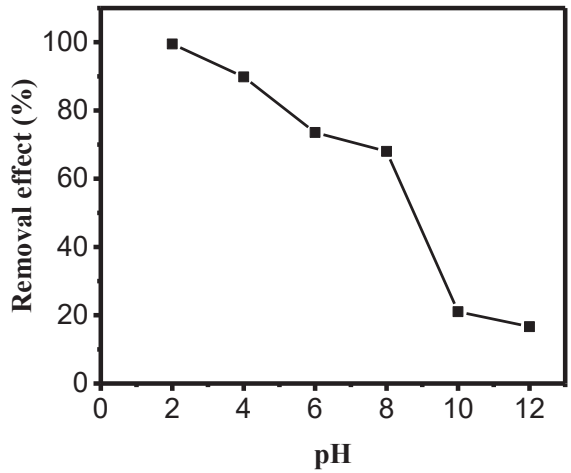


Figure 4: Effect of pH solution on adsorption of tartrazine.

The effect of initial pH solution on tartrazine adsorption on $MoS_2$ was carried out at various pH values from 2.0 to 12.0, which was adjusted by HCl 0.1M and NaOH 0.1M. The initial dye concentration and $MoS_2$ dosage were 20 mg/L and 0.08 g, respectively. Figure 4 shows the decrease in removal efficiency with pH solution. The removal efficiencies were 99.5%, 89.8%, 73.5%, 68.02%, 21.0% and 16.6% at pH values of 2.0, 4.0, 6.0, 8.0, 10.0, and 12.0, respectively. Some studies reported that the surface charge (zeta potential) of the $MoS_2$ has

negative when it is dispersed into water, and the value increases towards alkaline pH. [13, 14]. This leading to the increase of electrostatic repulsion between tartrazine of anion dye and the surface of $MoS_2$. Therefore, the adsorption rate and adsorption capacity decrease.

*Adsorption of different organic dyes on $MoS_2$*

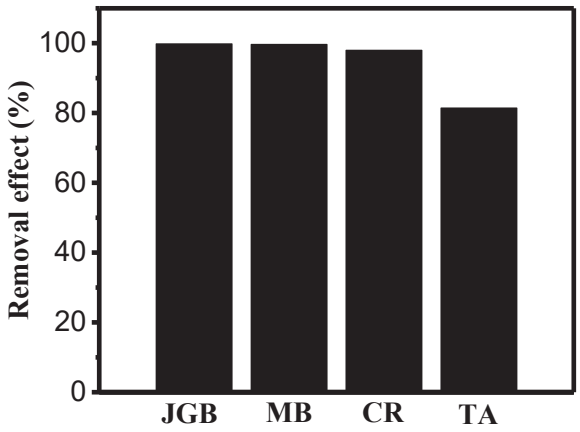


Figure 5: Effect of different organic dyes on the removal efficiency of $MoS_2$

The adsorption capacity of $MoS_2$ was also performed with various organic dyes such as tartrazine, nile blue, janus green B and congo red. All experiments were conducted at temperature of 30 $^oC$, dosage adsorpbent of 0.8 g/L, and dye concentration of 20 mg/L. The results are presented in Figure 5. It was seen that $MoS_2$ had a better adsorption of janus green B, methylene blue and congo red than that of tartrazine. The removal efficiencies in 60 min were 99.8, 99.7 and 97.9% for janus green B, methylene blue and congo red, respectively. These revealed that $MoS_2$ is the potential material for treating wastewater containing toxic organic substances.

*Adsorption kinetics*

Figure 6 (a) and (b) shows the pseudo-first order and pseudo-second-order plots for adsorption of tartrazine on $MoS_2$, respectively. Table 2 lists the rate constants, coefficient, calculated equilibrium adsorption capacity $q_{e,cal}$ and experimental equilibrium adsorption capacity $q_{e,exp}$ for tartrazine using above two kinetic models.

As shown in Table 2, the pseudo-second-order had the higher coefficient values ($R^2$ = 0,997) as compared to that of pseudo-first-order ($R^2$ = 0,891). The $q_e$ value (22.6 mg/L) calculated from the second-order-kinetic equation was close to the $q_e$ value (20.36 mg/L) experimentally calculated. This indicated that the pseudo-second-kinetic model better described the adsorption kinetics of tartrazine on $MoS_2$.

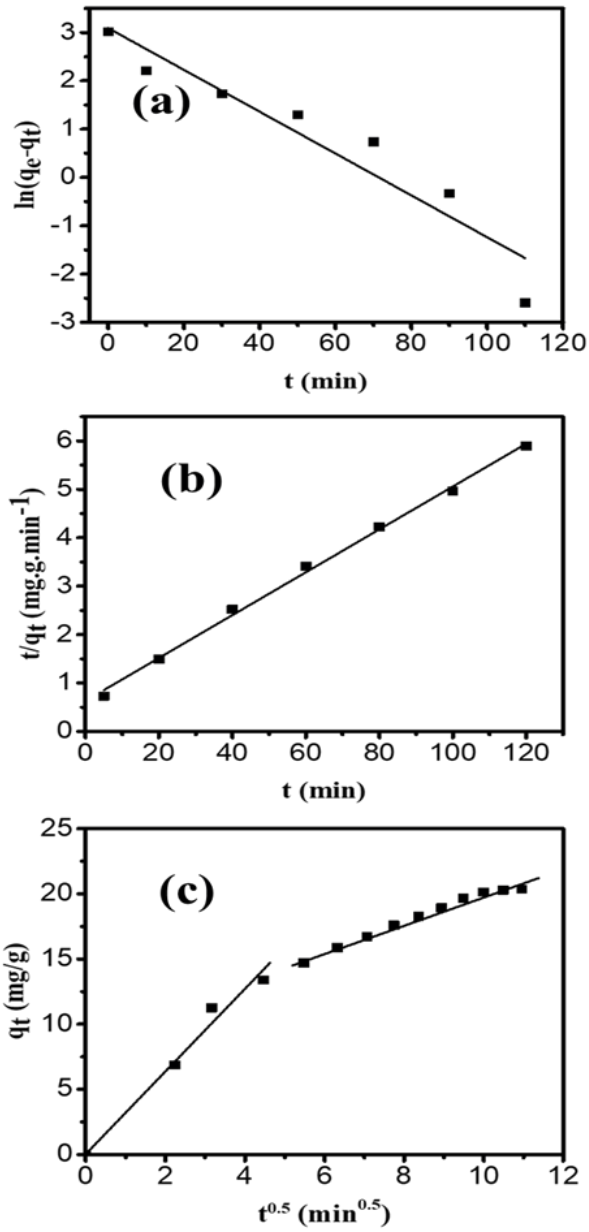


Figure 6: (a) Pseudo-first-order kinetics, (b) pseudo-second-order kinetics, and (c) intra-pacticle diffusion.

Figure 6 (c) showed the plot of $q_t$ versus $t^{0.5}$ for dye adsorption. The values of $k_i$ and C were obtained from the slope and intercept of plots of $q_t$ versus $t^{0.5}$, which were summarized in Table 2. Figure 6 (c) showed two linear graphs obtained from experimental data showing that the adsorption process was controlled by two steps. The first linear fraction (phase I) could be attributed to immediate use of the values available on the adsorbent surface. In contrast, the second linear fraction (phase II) could be attributed to the very slow diffusion of the substance that is slowly adsorbed from

http://doi.org/10.51316/jca.2020.076

the surface position into the internal void [15-17]. Therefore, during the adsorption on $MoS_2$, tartrazine molecules are adsorbed by the outer surface of the adsorbent at first. When the adsorbent on the outer surface reaches saturation, tartrazine molecules continue to enter the material's terminal holes. It can be seen in Table 2 that the $k_{i1}$ value is greater than the $k_{i2}$ value, which is understandable because the concentration of tartrazine remaining in the solution gradually decreases.

Table 2: Kinetics parameters for the adsorption of tartrazine on $MoS_2$.

| Dye | $q_{e,exp}$ | Pseudo-first-order model | | | Pseudo-secondorder model | | | Intra-pacticle diffusion | | | | | |
|---|---|---|---|---|---|---|---|---|---|---|---|---|---|
| Tartrazine | 20.36 | $q_{e,cal}$ | $k_1$ | $R^2$ | $q_{e,cal}$ | $k_2$ | $R^2$ | $C_1$ | $k_{i1}$ | $R^2$ | $C_2$ | $k_{i2}$ | $R^2$ |
| | | 22.02 | 0.0433 | 0.891 | 22.6 | 0.0031 | 0.997 | 0.212 | 3.11 | 0.980 | 9.08 | 1.08 | 0.982 |

## Conclusion

$MoS_2$ nano-corals were successfully synthesized via the hydrothermal method. The synthesized- material had large surface area and high pore volume, 83.9 $m^2/g$ and 0.48 $cm^3/g$. The performacne of the $MoS_2$ was evalutated by the adsorption of tartrazine. The result showed that the optimal $MoS_2$ dosage and equilibrium time of adsorption of tartrazine were 0.8 g/L and 120 min, respectively. Adsorption kinetic of TA adsorption onto $MoS_2$ has been investigated and the obtained results suggested that the pseudo-second order model can be used to describe the kinetics of adsorption. Furthermore, the $MoS_2$ material was also capable of good removal of various organic dyes in wastewater, suggesting its potential applications in water treatment.

### Acknowledgments

The authors are grateful for the financial support Vietnam National Foundation for Science and Technology Development (NAFOSTED) under grant number 104.05-2018.333.

## Reference

1. Tan, K.B., et al., Adsorption of dyes by nanomaterials: recent developments and adsorption mechanisms. Separation and Purification Technology, 150, (2015) 229-242. https://doi.org/10.1016/j.seppur.2015.07.009
2. Moussavi, G. and M. Mahmoudi, Removal of azo and anthraquinone reactive dyes from industrial wastewaters using MgO nanoparticles. Journal of hazardous materials, 168(2-3) (2009) 806-812. https://doi.org/10.1016/j.jhazmat.2009.02.097
3. Tu, V.A. and V.A. Tuan, A facile and fast solution chemistry synthesis of porous ZnO nanoparticles for high efficiency photodegradation of tartrazine. Vietnam Journal of Chemistry, 56(2) (2018) 214-219. https://doi.org/10.1002/vjch.201800016
4. Jeong, N., et al., Direct synthesis, characterization, and reverse electrodialysis applications of $MoS_2$ thin film on aluminum foil. Materials Characterization, 164 (2020) 110361. https://doi.org/10.1016/j.matchar.2020.110361
5. Wu, H., et al., An investigation on the lubrication mechanism of $MoS_2$ nano sheet in point contact: The manner of particle entering the contact area. Tribology International, 107 (2017) 48-55. https://doi.org/10.1016/j.triboint.2018.02.013
6. Ye, G., et al., Defects engineered monolayer $MoS_2$ for improved hydrogen evolution reaction. Nano letters, 16(2) (2016) 1097-1103. https:doi.org//10.1021/acs.nanolett.5b04331
7. Nazneen, A., et al., Structural, morphological, optical, and photocatalytic properties of Ag-doped $MoS_2$ nanoparticles. Journal of Molecular Structure, 1220 (2020) 128735. https://doi/.org/10.1016/j.molstruc.2020.128735
8. Wu, C., et al., Three-dimensional $MoS_2$/Carbon sandwiched architecture for boosted lithium storage capability. Nano Energy, 65 (2019) 104061. https://doi.org/10.1016/j.nanoen.2019.104061
9. Kallel, F., et al., Sorption and desorption characteristics for the removal of a toxic dye, methylene blue from aqueous solution by a low cost agricultural by-product. Journal of Molecular Liquids, 219 (2016) 279-288. https://doi.org/10.1016/j.molliq.2016.03.024
10. Yuan, Y.-J., et al., Visible-light-driven hydrogen production from water in a noble-metal-free system catalyzed by zinc porphyrin sensitized $MoS_2$/ZnO. Dyes and Pigments, 123 (2015) 285-292. https://doi.org/10.1016/j.dyepig.2015.08.014
11. Park, J.H., et al., Comparative sorption of Pb and Cd by biochars and its implication for metal immobilization in soils. Water, Air, & Soil Pollution, 224(12) (2013) 1711. https://doi.org/10.1007/s11270-013-1711-1
12. Maugé, F., et al., FT-IR study of surface properties of unsupported $MoS_2$. Catalysis today, 70(1-3) (2001) 271-284. https://doi.org/10.1016/S0920-5861(01)00423-0
13. Han, S., et al., Superior adsorption and regenerable dye adsorbent based on flower-like molybdenum disulfide nanostructure. Scientific Reports, 7 (2017) 43599. https://doi.org/10.1038/srep43599

14. Qiao, X.-Q., et al., Equilibrium and kinetic studies on MB adsorption by ultrathin 2D $MoS_2$ nanosheets. Rsc Advances, 6(14) (2016) 11631-11636. https://doi.org/10.1039/C5RA24328A
15. Ai, L. and Y. Zeng, Hierarchical porous NiO architectures as highly recyclable adsorbents for effective removal of organic dye from aqueous solution. Chemical engineering journal, 215 (2013) 269-278. https://doi.org/10.1016/j.cej.2012.10.059
16. Cheng, B., et al., Synthesis of hierarchical $Ni(OH)_2$ and NiO nanosheets and their adsorption kinetics and isotherms to Congo red in water. Journal of hazardous materials, 185(2-3) (2011) 889-897. https://doi.org/10.1016/j.jhazmat.2010.09.104
17. Zare, K., et al., Enhanced removal of toxic Congo red dye using multi walled carbon nanotubes: kinetic, equilibrium studies and its comparison with other adsorbents. Journal of Molecular Liquids, 212 (2015) 266-271. https://doi.org/10.1016/j.molliq.2015.09.027